Structure of liquid K-Pb alloys

1989 J. Phys.: Condens. Matter 1 5229

(http://iopscience.iop.org/0953-8984/1/31/022)

J. Phys.: Condens. Matter **1** (1989) 5229–5241. Printed in the UK

Structure of liquid K–Pb alloys

H T J Reijers, W van der Lugt†, C van Dijk‡ and M-L Saboungi§

† Solid State Physics Laboratory, Materials Science Centre, University of Groningen, Melkweg 1, 9718 EP Groningen, The Netherlands

‡ Netherlands Energy Research Foundation ECN, PO Box 1, 1755 ZG Petten, The Netherlands

§ Chemical Technology Division, Argonne National Laboratory, Argonne, Illinois 60439-4837

Received 17 January 1989

Abstract. The structure factors of liquid Pb, $K_{0.25}Pb_{0.75}$, $K_{0.50}Pb_{0.50}$, $K_{0.65}Pb_{0.35}$ and $K_{0.80}Pb_{0.20}$ have been measured by means of neutron diffraction. The main peaks of the structure factors of the alloys are preceded by a pre-peak which is most pronounced in $K_{0.50}Pb_{0.50}$. This pre-peak indicates that there is considerable ordering in the alloys, although there is also evidence for a tendency towards phase separation in at least one of the alloys. From inspection of the radial distribution functions it follows that Pb clusters are formed, the concentrations of which increase when the equi-atomic composition is approached. A simple model of the structure of $K_{0.50}Pb_{0.50}$ based on the reference interaction site model proves to be in excellent agreement with the measured structure factor.

1. Introduction

In recent years the K–Pb system has been studied extensively. The measurements made include resistivity (Meijer *et al* 1985), density (Saar and Ruppersberg 1988), the Darken excess stability function and the entropy of mixing (Saboungi *et al* 1986) and heat capacity (Johnson and Saboungi 1987). Recently, the structure of liquid $K_{0.50}Pb_{0.50}$ has been studied by means of neutron diffraction using a pulsed source by Saboungi *et al* (1987). They found a large and narrow pre-peak at 0.96 $Å^{-1}$, which in their work is referred to as the first sharp diffraction peak. The phase diagram has been determined by Meijer *et al* (1985) and is shown in figure 1. The resistivity of the alloys exceeds the range of typical metallic values, whereas the densities, the excess stabilities, the entropies of mixing and the specific heat capacities show deviations from ideal solutions. These results have in common that the anomalous behaviour is strongest at the equi-atomic composition.

Similar anomalous behaviour has been found in other binary alloys of alkali metals, on the one hand, and group IVa elements on the other, though not necessarily at the equi-atomic composition. For example, in the Li–Pb system the anomalous effects are strongest at the composition of 80 at.% Li. More generally, alloys are said to form compounds in the liquid state at the composition(s) at which the anomalous behaviour occurs (Van der Lugt and Geertsma 1987). The primary cause of this phenomenon is the large difference in electro-negativity between members of these two groups (1.85 V for K–Pb on the Miedema scale). Consequently, alloying of two metals from both groups is accompanied by a considerable charge transfer from the less to the more electro-negative element. This leads to alloys with strong ionic character.

0953-8984/89/315229 + 13 $02.50

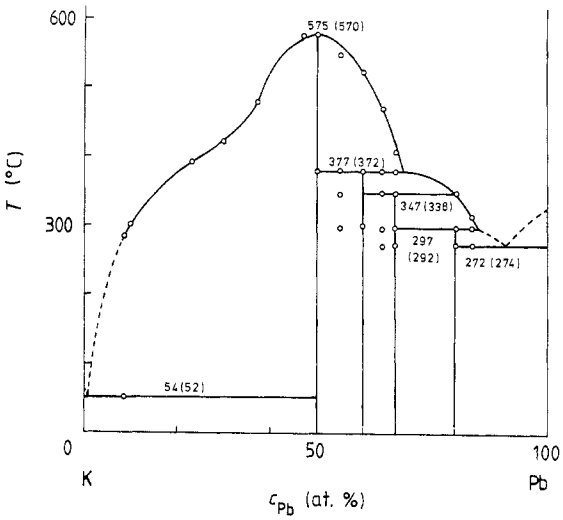

Figure 1. Phase diagram of the K–Pb system determined by Meijer *et al* (1985).

By comparing the resistivities (Meijer *et al* 1985) or the Darken excess stability functions (Saboungi *et al* 1986) of liquid Li–Pb, Na–Pb and K–Pb, a shift in stoichiometry is observed. Whereas liquid Na–Pb, just as Li–Pb, forms an octet compound $Na_{0.80}Pb_{0.20}$, the K–Pb system forms only an equi-atomic compound $K_{0.50}Pb_{0.50}$. The octet compound can still be understood by application of simple chemical valence rules. This is no longer the case for equi-atomic compounds. Analysis of the electronic transport properties and band structure calculations (Geertsma *et al* 1984, Springelkamp *et al* 1985, Van der Lugt and Geertsma 1987) has led to the assumption that poly-anions consisting of $(Pb_4)^{4-}$ tetrahedra, the so-called Zintl ions (Busmann 1961), are formed in liquid K–Pb that are responsible for the shift in stoichiometry from 80 to 50 at.% alkali metal. Whenever we speak of Pb clusters in the remainder of this paper, we mean these $(Pb_4)^{4-}$ tetrahedra.

Recently, the formation of poly-anions has also been observed by Barnes and Enderby (1988) in liquid $Cu_{0.50}Se_{0.50}$. Employing the method of isotopic substitution, they were able to determine the partial structure factors. The Se–Se partial distribution function provides clear evidence that $(Se_2)^{2-}$ ions exist in the liquid.

The hypothesis that $(Pb_4)^{4-}$ ions persist in the liquid is also suggested by the crystal structure of $K_{0.50}Pb_{0.50}$, which was shown to be isomorphous to that of $Na_{0.50}Pb_{0.50}$ (Hewaidy *et al* 1964). According to Marsh and Shoemaker (1953), who have investigated the crystal structure of $Na_{0.50}Pb_{0.50}$ in detail, the structure is tetragonal with space group $D_{4h}^{20}(I4_1/acd)$. Application of Rietveld analysis to a recently determined powder-diffraction pattern of $K_{0.50}Pb_{0.50}$ (Richardson 1987) has yielded: $a = 11.5368$ Å and $c = 18.8689$ Å. The unit cell contains 32 K and 32 Pb atoms. The Pb atoms are arranged in eight nearly regular tetrahedra surrounded by shells of K atoms. The shell of K atoms enclosing each Pb_4 tetrahedron contains 16 K atoms, each of which belongs also to shells surrounding other Pb_4 tetrahedra. From the Rietveld analysis follows that the average Pb–Pb bond length is 3.1182 Å, while the average K–Pb and K–K bond lengths are respectively 3.8011 and 4.0071 Å.

Given this experimental and theoretical information we decided to perform neutron-diffraction measurements to investigate the composition dependence of the structure of liquid K–Pb, and, more particularly, to search for further evidence for the existence of Pb_4 tetrahedra as structural entities. Part of the results presented here has already been published elsewhere (Reijers *et al* 1987).

2. Experimental

The neutron diffraction measurements were carried out on HB1 of the High Flux Reactor at ECN in Petten. A bent monochromator crystal of pyrolytic graphite was used to select two wavelengths (1.24 Å and 2.55 Å). A pyrolytic-graphite filter was placed in the incident beam to reduce the higher-order wavelength contamination of the 2.55 Å radiation. The spectrometer was equipped with a movable linear-position-sensitive ^{3}He detector operating at a pressure of 5 atm. This consists of two tubes, 50 cm in length, placed one above the other in such a way that the angular ranges overlap slightly. The total effective aperture is 39°. The signals from the detector are divided over 256 channels, each representing a detector element of 4 mm length, and are stored in a multi-channel analyser.

A temperature-controlled furnace was used. The heating element consists of a Mo resistance wire (total resistance: 15 Ω), vertically wound back and forth between two aluminium oxide spacers. The spacers are held in position by a cylindrical Mo heat shield, that is surrounded by a second heat shield. A chromel–alumel thermocouple is used to measure the temperature of the sample, while a platinel-II thermocouple feeds back the registered temperature to the power supply. The output of the power supply is adjusted to maintain a constant temperature. Because of a gradient, the temperature varied within 5 °C of the set temperature over the length of the sample. The furnace was placed in an aluminium vessel that was evacuated to a pressure lower than 10^{-4} Torr. The maximum attainable temperature was 750 °C, for which 4.5 kW was required.

To reduce background scattering, a large triangular shield was made and placed in front of the detector. However, this proved to be insufficient to eliminate contamination caused by Bragg peaks arising from the various parts of the furnace that are hit by the incident beam. So two pieces of Gd foil, 100 μm thick, were used to prevent spurious radiation entering the detector. Since Gd is a very poor thermal conductor (Gschneider 1961), this did not result in a serious heat leakage (around 0.01% of the input power was lost in this way).

The sample containers were constructed from $Ti_{0.07}Zr_{0.33}$. This alloy combines the advantage of being a zero alloy with that of having an excellent resistance against corrosive-liquid alloys. Although in this alloy a slight tendency for chemical short-range order has been found by Yarnell *et al* (1973), this does not disturb the measurements. The material yields a smooth background that can be easily subtracted out. The sample containers had an inner diameter of 20 mm, a wall thickness of 0.5 mm and a height of 60 mm.

The K–Pb samples were prepared in a helium-filled glove box, in which the oxygen level was less than 1 ppm. Lead ingots of a nominal purity of 99.999% were commercially obtained from Alfa Ventron Inc., and potassium was delivered in glass ampoules by Kawecki and had a nominal purity of 99.9998%. The alloys for which $c_{Pb} \geq 0.5$, where c_{Pb} is the concentration of Pb, were prepared by alloying the appropriate amounts of the pure metals in a stainless-steel crucible and by subsequent quenching of the liquid alloy on a copper plate. The crystallised pieces of alloy were hard and brittle, and could easily be crushed into smaller fragments. After that, the pieces were put, one by one, into the sample container, which was kept at a temperature greatly exceeding the melting point. Adding the sample piece by piece prevented helium bubbles forming in the sample during filling. This procedure could not be used for the K-rich alloys because they stuck to the copper plate after quenching. Besides, they are soft, so cannot be crushed. Therefore these alloys had to be prepared *in situ*. The sample depth when in the

containers was 4 cm. After being filled, the containers were closed tightly, using a Helicoflex ring (type HN120, manufactured by Péchiney Ugine Kuhlmann). Sealing action is made possible by tightening a screw that draws a bolt upwards that in turn presses the Helicoflex ring radially outwards against the inner wall of the container. This part of the inner wall, as well as the bolt and screw, was made from Nimonic, a specially designed alloy with excellent mechanical properties that are preserved at elevated temperatures up to 800 °C. The torque applied to the screw ranged from 35 to 50 Nm, depending on the temperature desired.

In a typical run, the detector was set at different angles ($\varphi = 25°, 45°, 65°$ and 85° for 2.55 Å, $\varphi = 54°, 72°$ and 90° for 1.24 Å, φ being the angle between the centre of the detector and the transmitted beam), to cover a sufficiently large angular range. The detector stayed at a specified angle until a fixed number of neutrons had been counted by the monitor placed between monochromator and sample. After that, it was moved to another angle. For the longer wavelength it took 20 hours, for the shorter one 8 hours to complete a run. For the $K_{0.50}Pb_{0.50}$ specimen this amounts to an average intensity of 70000 and 15000 counts per channel for 1.24 Å and 2.55 Å respectively. Apart from the sample runs, we also performed an empty container run, and a run wherein the container was replaced by a Cd rod of the same dimensions. Both these runs took place under the same conditions as the sample runs. They were used to correct the intensities of the sample runs for container and background scattering. Two separate runs were made to calibrate the spectrometer. In one, the intensity of an incoherent scatterer was measured to find the relative counting efficiency of the channels. In the other, the (non-linear) relation between channel number and the angle subtended by the corresponding detector element, the goniometer axis and the centre of the detector, was determined.

3. Data reduction

We will discuss briefly the corrections that have been used to derive the structure factor from the raw data. More details can be found in Ruppersberg and Egger (1975) and Alblas *et al* (1983). First, the raw data were corrected for small variations in counting efficiency over the length of the detector. The data, being still a function of channel number and detector position, were subsequently converted into intensities that depended only on the scattering angle. Next, the measured intensities of the sample were corrected for container scattering and background scattering, according to the procedure developed by Poncet (1976, 1977). After that, the data were interpolated on a constant-q grid ($\Delta q = 0.014$ Å^{-1}) and were corrected for multiple scattering (Blech and Averbach, 1965), incoherent scattering and inelastic scattering (Yarnell *et al* 1973, Placzek 1952). As to the last correction, we have assumed the following approximation for the wavelength-dependence of the detector efficiency:

$$\varepsilon(\lambda) = 1 - A \exp(-B\lambda/2\pi) \tag{1}$$

with $A = 0.9387$ and $B = 3.532$ Å^{-1}. In the wavelength range from 1 to 3 Å this differs by less than 1% from the exact result (see Alblas *et al* 1983). The data were extrapolated to $q = 0$ by fitting a parabola $C_1 + C_2q^2$ to the low-q part (Pings 1968). Finally, the corrected data were normalised to find the scattered intensity per atom, $I_a^{coh}(q)$, and from that the structure factor defined as

$$S(q) = I_a^{coh}(q)/4\pi\langle b^2\rangle \tag{2}$$

where b is the scattering length of a component averaged over the isotopes and nuclear

spin states and where $\langle \ldots \rangle$ denotes an average over the concentrations of the components. Each wavelength requires its own normalisation factor. The two normalisation factors were chosen in such a way that, on average, $S(q)$ had the same value for both wavelengths in the q range where the experimental data overlapped, and that simultaneously the discrete form of the following sum rule (Wagner 1978) was fulfilled:

$$\sum_{j=1}^{N} q_j^2 (S(q_j) - 1)\, \Delta q = -2\pi^2 \rho_0 \tag{3}$$

where N is the total number of data points ($N = 570$) and ρ_0 is the particle number density derived from the data of Saar and Ruppersberg (1987).

The structure factor was Fourier-transformed to obtain the radial distribution function $N(r)$, defined as

$$N(r) = 4\pi r^2 \rho_0 + \frac{2}{\pi} r \frac{\langle b^2 \rangle}{\langle b \rangle^2} \int_0^{q_{\max}} q(S(q) - 1) \sin(qr)\, \mathrm{d}q. \tag{4}$$

Using only the $S(q)$ data up to the maximum experimentally accessible q value (8 Å^{-1}), led to spurious ripples in the radial distribution function. Therefore, we have extrapolated the $S(q)$ data by using a suitable extrapolation function. For pure Pb a satisfactory fit was obtained by using the four-parameter function due to Verlet (1968):

$$S(q) = 1 + (C/q) \exp(-Dq) \cos(Aq + B) \tag{5}$$

where A, B, C and D are adjustable parameters. This is, apart from an additional fifth parameter, the same function as has been applied by Dahlborg *et al* (1977) to fit the high-q part of their structure factor of liquid Pb. For the K–Pb alloys where molecular species were to be expected, we used the spherical average of the limiting form of the structure factor of a molecule (Gubbins *et al* 1973) the smallest bond of which is characterised by the distance d:

$$S(q) = 1 + (P/q) \exp(-(Rq)^2) \sin(qd)/(qd) \tag{6}$$

where the parameters P, R and d are found by adjustment. Note that upon Fourier-transformation of $q(S(q) - 1)$ with $S(q)$ given by (6), a Gaussian function is obtained centred at $r = d$ and of width R. The above functions were fitted to the $S(q)$ data between 3.5 and 8 Å^{-1}. The accuracy of the fits is rather good. The deviation of the data from the fitted points is 1.5% per point, on average. The structure factors were subsequently extrapolated up to 20 Å^{-1}.

4. Results and discussion

4.1. Structure factors and radial distribution functions

Figures 2(*a–e*) show the structure factors (SFs) of Pb, $K_{0.25}Pb_{0.75}$, $K_{0.50}Pb_{0.50}$, $K_{0.65}Pb_{0.35}$ and $K_{0.80}Pb_{0.20}$ measured at temperatures slightly above the melting points (340 °C for Pb, 385 °C for $K_{0.25}Pb_{0.75}$, 585 °C for $K_{0.50}Pb_{0.50}$, 500 °C for $K_{0.65}Pb_{0.95}$ and 400 °C for $K_{0.80}Pb_{0.20}$), figures 3(*a–e*) the radial distribution functions (RDFs) that have been found by Fourier-transformation of the extrapolated SFs (see § 3). For comparison, the SF and RDF of liquid K measured by Huijben and Van der Lugt (1979) have also been included (figures 2(*f*) and 3(*f*)). The scattering lengths used for the calculations were taken from a compilation by Koester and Yelon (1982).

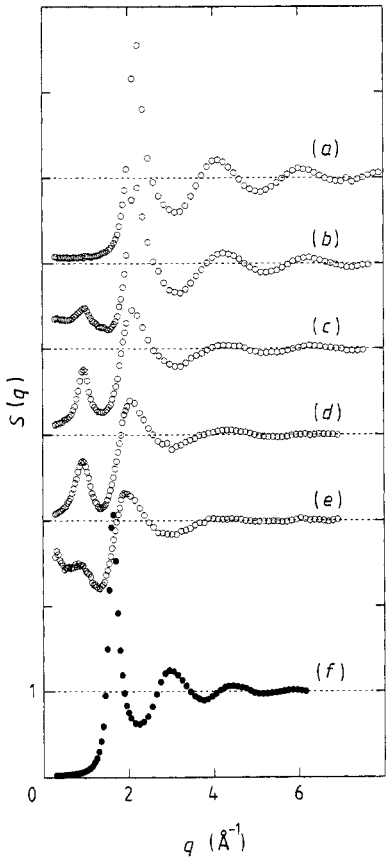

Figure 2. Measured structure factors of (*a*) Pb at 340 °C (*b*) $K_{0.25}Pb_{0.75}$ at 385 °C, (*c*) $K_{0.50}Pb_{0.50}$ at 585 °C, (*d*) $K_{0.65}Pb_{0.35}$ at 500 °C, (*e*) $K_{0.80}Pb_{0.20}$ at 400 °C, and (*f*) K at 65 °C.

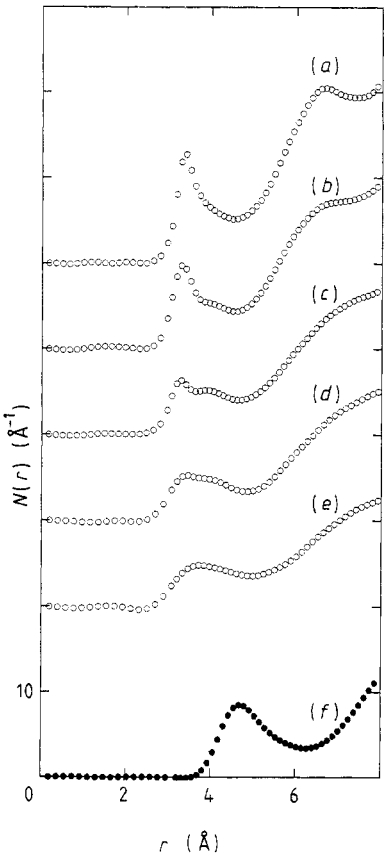

Figure 3. Radial distribution functions found by Fourier-transformation of the structure factors to the left of them.

Table 1. Comparison of measured structure factors of liquid Pb.

		1st maximum		2nd maximum		3rd maximum	
Reference	*t* °C	*q* (Å^{-1})	*S*(*q*)	*q* (Å^{-1})	*S*(*q*)	*q* (Å^{-1})	*S*(*q*)
Kaplow *et al* (1965)	329	2.19	2.78	4.11	1.30	6.09	1.10
North *et al* (1968)	340	2.23	2.60	4.20	1.34	6.04	1.10
Waseda *et al* (1975)	340	2.28	2.46	4.23	1.29	6.17	1.11
Steffen *et al* (1976)	350	2.20	2.66	4.10	1.29	6.05	1.11
Dahlborg *et al* (1977)	340	2.21	2.79	4.10	1.30	6.05	1.13
Present work	340	2.19	2.61	4.10	1.21	6.06	1.10

Let us first discuss the results for pure Pb. The SF of liquid Pb has frequently been investigated. Table 1, partly taken from Dahlborg *et al* (1977), summarises some of the results obtained by various authors. From this table it follows that our data agree quite satisfactorily with those of other measurements. By fitting a Gaussian function to the first peak of the RDF, we find a nearest-neighbour distance of 3.39 Å and a coordination number of 7.4. These values agree well with those reported by Waghorne *et al* (1967):

3.40 Å and 8.0 respectively. Applying the same procedure to the second coordination shell yields a distance of 6.75 Å.

Turning now to the SFs of the alloys, we see that both the main peak, i.e. the peak at about 2 $Å^{-1}$, and the high-q oscillations change continuously in going from Pb to K. However, unlike that which occurs with the SFs of the pure components, a pre-peak appears in front of the main peak in the SFs of the alloys. Although its position, 0.97 $Å^{-1}$, remains unaltered (within the experimental accuracy) as a function of composition, its height varies strongly. The maximum height is attained at the equi-atomic composition. At this composition one can also distinguish a shoulder at the right-hand side of the main peak. Both the pre-peak and the shoulder reveal important structural aspects. The shoulder is, following the arguments given by Alblas *et al* (1983) and Reijers *et al* (1987), interpreted as an indication for the existence of small structural units. Thus the shoulder supports the assumption (Geertsma *et al* 1984) that $(Pb_4)^{4-}$ ions persist in the liquid alloy. From the presence of the pre-peak it follows that K atoms dominate among the neighbouring atoms of the Pb clusters. A simple approximating formula (Boos *et al* 1972) that converts the prepeak position to a distance in real space yields 7.96 Å. In the solid, this distance varies from 7.42 to 8.03 Å, so that our value can be considered as an average inter-cluster separation. The SF of $K_{0.80}Pb_{0.20}$ shows, in addition to the pre-peak, a large small-angle scattering. This will be discussed in the next section. The same effect, though weaker, is observed in $K_{0.25}Pb_{0.75}$.

Finally, we also performed measurements at higher temperatures† (500 °C for Pb, 585 °C for $K_{0.25}Pb_{0.75}$, 740 °C for $K_{0.50}Pb_{0.50}$, 600 °C for $K_{0.65}Pb_{0.35}$ and 500 °C for $K_{0.80}Pb_{0.20}$). The pre-peak and the shoulder become weaker as the temperature is increased. This indicates that the above-mentioned structural properties gradually disappear when the temperature rises.

To obtain information about the real-space structure we have determined the RDFs. We define the first coordination shell as lying approximately between 2.5 Å and the onset of the steep rise beginning, say, at 4.5–5 Å. The only alloy showing also a coordination shell beyond that, centred at 7 Å, is $K_{0.25}Pb_{0.75}$. Except for $K_{0.80}Pb_{0.20}$, two, more or less well-defined maxima, can be distinguished in the first coordination shell. The first maximum is at approximately the same position as the first peak in the RDF of pure Pb. This maximum becomes less distinct with increasing K concentration. The second maximum, next to the first maximum, shows up as a shoulder in $K_{0.25}Pb_{0.75}$ and $K_{0.65}Pb_{0.35}$, whereas in $K_{0.50}Pb_{0.50}$ a separate peak has clearly developed. In $K_{0.80}Pb_{0.20}$ both peaks together form a broad maximum. Here, we again find support for our hypothesis that Pb_4 tetrahedra exist. If K–Pb were simply a mixture of K and Pb atoms, the only driving force between the atoms being a tendency towards hetero-coordination, the first coordination shell would have shown one maximum only, as has been observed among others in the compound-forming alloys Au–Cs (Martin *et al* 1980) and Cs–Sb (Lamparter *et al* 1984). However, the fact that there are two preferred nearest-neighbour distances can point either to phase-separation or to the existence of clusters of atoms. In the former case, the two maxima correspond to the nearest-neighbour distances in either of the two phases. This has been observed in the Cs-rich compositions of the above-mentioned Au–Cs and Cs–Sb alloys. In the latter case, the two maxima characterise the intra- and extra-cluster distances, i.e. the distance between atoms within the same cluster and the distance between atoms not belonging to the same cluster. The latter group includes the distance between K atoms, the distance between unbound Pb atoms, the distance between Pb atoms each belonging to different tetrahedra, and the distance between a free K or Pb atom and a Pb atom in a tetrahedron. Evidently, for those

† These are not shown here. They can be supplied on request.

Table 2. Results of Gaussian fits to the two maxima in the coordination shell of the radial distribution function.

	1st peak			2nd peak		
	d_1 (Å)	σ_1 (Å)	A_1	d_2 (Å)	σ_2 (Å)	A_2
$K_{0.25}Pb_{0.75}$	3.322	0.260	5.836	4.078	0.294	3.617
$K_{0.50}Pb_{0.50}$	3.298	0.278	3.712	4.065	0.310	3.363
$K_{0.65}Pb_{0.35}$	3.390	0.359	3.848	4.167	0.307	2.583
$K_{0.80}Pb_{0.20}$	3.602	0.426	4.212	4.568	0.397	2.995

compositions for which $c_K \leqslant 0.65$, the possibility of phase separation must be excluded here since, at least up to $c_K = 0.65$, K–Pb is a strongly compound-forming alloy. Thus we are led to the conclusion that the double-peak structure is due to the presence of clusters.

We have fitted two Gaussian functions to the two maxima in the following way. The first Gaussian function was fitted to the leading edge of the total RDF. The fitted function was subsequently subtracted from the RDF and another Gaussian function was fitted to the net result. Table 2 gives the distances d_k around which the peaks are centred, the half widths σ_k of the peaks and the areas A_k under the peaks. The values of d_1, d_2 and A_1 show all the same trend. From $K_{0.25}Pb_{0.75}$ to $K_{0.50}Pb_{0.50}$ they decrease, reaching a minimum value for the equi-atomic composition, and from $K_{0.50}Pb_{0.50}$ onwards to the K-rich alloys they increase again.

As has been argued above, the main contribution to the first maximum comes from intra-cluster Pb–Pb correlations. Assuming that this is the only contribution, the coordination number of Pb atoms within a cluster can be calculated. The partial coordination numbers $N_{ij}^{(k)}$, where $N_{ij}^{(k)}$ is the number of j-type atoms surrounding an i-type atom in the k-th maximum of the first coordination shell, are related to A_k as follows:

$$A_k = \sum_{i,j} w_{ij}/c_j \, N_{ij}^{(k)}. \tag{7}$$

The weights w_{ij} are given by

$$w_{ij} = c_i c_j \, b_i b_j / \langle b \rangle^2. \tag{8}$$

Table 3 gives the weights and the partial coordination numbers $N_{PbPb}^{(1)}$. If all Pb atoms were arranged in tetrahedra, the first maximum should give $N_{PbPb}^{(1)} = 3$. In table 3 one sees that it is always larger than this value. Similarly, where we compare d_1 with the

Table 3. Weights of the partial radial distribution functions and partial coordination numbers.

	w_{KK}	w_{KPb}	w_{PbPb}	$N_{PbPb}^{(1)}$	$N_{KPb}^{(2)}$
$K_{0.25}Pb_{0.75}$	0.0133	0.2038	0.7830	5.59	13.31
$K_{0.50}Pb_{0.50}$	0.0788	0.4039	0.5173	3.59	4.16
$K_{0.65}Pb_{0.35}$	0.1766	0.4873	0.3361	4.01	—
$K_{0.80}Pb_{0.20}$	0.3716	0.4760	0.1524	5.52	—

Pb–Pb distance within a tetrahedron in the crystal (3.1182 Å), we find that, for all alloys, d_1 is larger than this distance. From the alloys investigated the values $N_{PbPb} = 3$ and $d_1 = 3.1182$ Å are best approached by $K_{0.50}Pb_{0.50}$, so that we conclude that in this system the concentration of Pb_4 tetrahedra relative to the total concentration of Pb atoms is the largest.

To derive partial coordination numbers from the second maximum is more difficult, because it consists of contributions of various extra-cluster distances. Comparing the weights we can, to first approximation, neglect the K–K contribution for $K_{0.25}Pb_{0.75}$ and $K_{0.50}Pb_{0.50}$. For these systems we have calculated $N^{(2)}_{KPb}$ under the assumption that only K–Pb correlations contribute (see table 3). For $K_{0.25}Pb_{0.75}$, $N^{(2)}_{KPb}$ is too large, probably due to the neglect of the contribution of Pb–Pb correlations. The value calculated for $K_{0.50}Pb_{0.50}$ on the other hand is lower than in the crystal structure. In the crystal we have $N_{KPb} = 7$. Besides, the average K–Pb distance is smaller in the crystal (3.8011 Å) than the value of d_2 in the liquid (4.065 Å).

4.2. Zero-wavevector limit

The SF of $K_{0.80}Pb_{0.20}$ shows an increase towards small q values. Also, the SF of $K_{0.75}Pb_{0.25}$ does not converge to the typical small values associated with a zero-wavevector limit determined only by the compressibility. On the other hand, no increase for $q \rightarrow 0$ has been found for $K_{0.50}Pb_{0.50}$ and $K_{0.65}Pb_{0.35}$. Unfortunately, the smallest experimentally attainable q value, 0.3 Å^{-1}, is rather large for making a reliable extrapolation to $q = 0$. Consequently, we do not give numerical values of the zero-wavevector limit of the SFs. Instead we will discuss the small-angle scattering of both $K_{0.80}Pb_{0.20}$ and $K_{0.25}Pb_{0.75}$ in a qualitative way.

In the case of alloys, a large zero-wavevector limit indicates a tendency towards phase separation, i.e. large concentration fluctuations. Additional evidence for this can be found in the phase diagram (figure 1). In the range between 10 and 30 at.% Pb and in the range between 70 and 90 at.% Pb, the liquidus curve is relatively flat and shows hardly any curvature. This too reflects a tendency towards two-liquid immiscibility (Geertsma 1985). We have already noted that a pre-peak can also be observed in the SFs of both $K_{0.80}Pb_{0.20}$ and $K_{0.25}Pb_{0.75}$. This pre-peak can be assumed to be a faint remnant of the pre-peak in the SF of $K_{0.50}Pb_{0.50}$. The combination of pre-peak and tendency towards phase separation implies that there will be a K–Pb phase dominated by Pb_4 clusters surrounded by K atoms as in $K_{0.50}Pb_{0.50}$, whereas the other phase consists mainly of K atoms for $K_{0.80}Pb_{0.20}$ or Pb atoms for $K_{0.25}Pb_{0.75}$.

The picture given above of $K_{0.80}Pb_{0.20}$ being separated into a phase having the structural properties of the equi-atomic alloy and a phase containing the remaining alkali atoms, is in fact very similar to the behaviour of metal–salt mixtures like K–KCl. The phase diagram of K–KCl is characterised by a large miscibility gap (Bredig 1964) and its SF shows a strong small-angle scattering in K-rich compositions (Jal *et al* 1988). Both phenomena are a consequence of a tendency towards formation of salt-like and metal-like regions. Another system having similar behaviour is liquid Au–Cs. This alloy is known to form a compound of ionic character at the equi-atomic composition, whereas in the Cs-rich alloys a strong small-angle scattering is observed (Martin *et al* 1980 p 49). This has been explained by Martin *et al* (1980 p 61) by assuming that the Cs-rich alloys consist, over a time-average, of ionic AuCs regions and metallic Cs regions.

Returning now to K–Pb, in terms of chemical thermodynamics the presence of concentration fluctuations in the concentration range between the pure metal and the

equi-atomic compound are an indication of the high stability of the latter. Inspection of the phase diagram of many alkali group III and alkali group IV systems (Thümmel and Klemm 1970, Tamaki and Cusack 1979) shows that it must be a rather common phenomenon.

4.3. RISM-calculations

Finally, we have tried to model the SF of $K_{0.50}Pb_{0.50}$ using the reference interaction site model (RISM) proposed by Chandler and Andersen (1972) to describe pair-correlation functions in molecular systems. They solved the generalised Ornstein–Zernike equation by assuming that the direct correlation function between two molecules can be approximated by the sum of direct correlation functions between the interaction sites, i.e. the individual atoms of which the molecules consist. A numerical procedure to solve the RISM equations was developed by Lowden and Chandler (1973), who applied RISM to, among others, liquid CCl_4, CS_2 and C_6H_6 (1974).

The total SF in RISM is defined as

$$S(q) = \sum_{\alpha,\gamma} b_\alpha b_\gamma (\omega_{\alpha\gamma}(q) + \rho_m h_{\alpha\gamma}(q)) \Big/ \sum_\alpha b_\alpha^2 \tag{9}$$

where ρ_m is the density of molecules, $\omega_{\alpha\gamma}(q)$ is the Fourier-transform of the pair-correlation function between sites α and γ of the same molecule and $h_{\alpha\gamma}(q)$ is that between sites α and γ of different molecules. Taking into account the fact that the atoms vibrate around their equilibrium position inside the molecules, $\omega_{\alpha\gamma}(q)$ can be written as

$$\omega_{\alpha\gamma}(q) = (\sin(qd_{\alpha\gamma})/qd_{\alpha\gamma}) \exp(-\tfrac{1}{2}(q\Delta d_{\alpha\gamma})^2) \tag{10}$$

where $d_{\alpha\gamma}$ is the equilibrium distance between sites α and γ, and $\Delta d_{\alpha\gamma}$ is the root-mean-square fluctuation in $d_{\alpha\gamma}$. According to the definition of Ashcroft and Langreth (1967), the total SF can be written as a linear combination of partial SFs $S_{ij}(q)$ as follows:

$$S(q) = \sum_{i,j} (c_i c_j)^{1/2} (b_i b_j / \langle b^2 \rangle) S_{ij}(q) \tag{11}$$

where i and j denote the type of atom and c_i and c_j are the corresponding concentrations. By combining (9) and (11) the expressions for the partial SFs and, upon Fourier-transformation, for the partial RDFs can be derived:

$$S_{ij}(q) = \frac{1}{n(c_i c_j)^{1/2}} \sum_{\alpha=i,\gamma=j}^{m} (\omega_{\alpha\gamma}(q) + \rho_m h_{\alpha\gamma}(q)) \tag{12}$$

and

$$N_{ij}(r) = \frac{1}{nc_i c_j} 4\pi r^2 \rho_0 \frac{\langle b^2 \rangle}{\langle b \rangle^2} \left(\sum_{\substack{\alpha=i,\gamma=j \\ \alpha \neq \gamma}}^{m} \omega_{\alpha\gamma}(r) + \rho_0 \sum_{\alpha=i,\gamma=j}^{m} h_{\alpha\gamma}(r) \right). \tag{13}$$

Here n is the number of atoms in a molecule. The notation $\alpha = i$ ($\gamma = j$) means that the summation is only over those sites $\alpha(\gamma)$ that are of type $i(j)$. The functions $\omega_{\alpha\gamma}(r)$ and $h_{\alpha\gamma}(r)$ are the Fourier-transforms of $\omega_{\alpha\gamma}(q)$ and $h_{\alpha\gamma}(q)$ respectively.

Rather than using a mixture of alkali atoms and tetrahedra as Alblas did for the Na–Sn system (Alblas *et al* 1983), we have invoked a single-structural unit for RISM that was motivated by the crystal structure of $K_{0.50}Pb_{0.50}$. This unit was originally proposed by

Saboungi *et al* (1987). In solid $K_{0.50}Pb_{0.50}$ the Pb atoms are arranged in nearly regular tetrahedra, surrounded by 16 K atoms. Four of these K atoms are positioned approximately opposite the centres of the faces of the Pb_4 tetrahedra. On the basis of this information, a structural unit consisting of two regular interlocking tetrahedra of different size has been constructed. The smaller tetrahedron has the Pb atoms at its corners, the larger one the K atoms. The positions of the K atoms in the structural unit are taken to be the same as in the crystal. As has been noted by Van der Lugt and Meijer (1987) and by Van der Lugt and Geertsma (1987), these positions correspond with the ones that are favoured because of the electron distribution: electron clouds protrude from the Pb_4 tetrahedra at the side-faces, accommodating the stripped K atoms. In figure 4(*d*), the measured and calculated SF are plotted together. The following set of parameters has been used for the RISM calculations: $d = 3.1182$ Å, $D = 6.5702$ Å, $\sigma_K = 3.0$ Å, $\sigma_{Pb} = 4.0$ Å, $\Delta d_{PbPb} = 0.2$ Å, $\Delta d_{KK} = 0.4$ Å, $\Delta d_{KPb} = 0.4$ Å and $\rho_m = 0.0027$ Å^{-3}, where d and D are the lengths of the sides of the smaller and larger tetrahedra respectively, σ is the hard sphere radius and the Δd_{ij}s are the root-mean-square fluctuations. The distances were derived from the crystal structure data and ρ_m was calculated from the measured density of liquid $K_{0.50}Pb_{0.50}$ (Saar and Ruppersberg 1988). The remaining parameters were found by adjustment.

The correspondence between the two SFs is rather good, except for the height of the pre-peak which is greater in the calculated than in the measured $S(q)$. Additional calculations involving free K and Pb atoms have shown that this is a consequence of our assumption that all atoms are arranged in structural units. However, the neutron-diffraction measurements of Saboungi *et al* (1987) showed a much higher pre-peak than our measurements. At present, it is not clear what this difference is caused by. A similar discrepancy has been found in the SFs of CCl_4 that were measured using reactor and pulsed-neutron sources (Bermejo *et al* 1988).

Inspection of the partials (figures 4(*a–c*)) reveals that the pre-peak is mainly caused by Pb–Pb correlations and also to a lesser degree by K–K correlations. The K–Pb partial has a minimum at the position of the pre-peak. In the first coordination shell of the total RDF (figure 5(*d*)) three maxima can be distinguished, the last two of which show up as only one peak in the measured RDF. From comparison with the partials (figures 5(*a–c*)) it follows that the first maximum is a Pb–Pb peak, the second consists of a mixture of K–Pb and K–K contributions, and the third peak is again due to Pb–Pb correlations. The following coordination numbers have been calculated from the partials: $N_{PbPb} = 3$, $N_{KPb} = 5$ and $N_{KK} = 4$. The values of N_{PbPb} and N_{KPb} agree well with the corresponding values found from the RDF of $K_{0.50}Pb_{0.50}$ (3.59 and 4.16 respectively).

5. Conclusion

Neutron diffraction measurements on a number of liquid K–Pb alloys indicate that among the alloys investigated the equi-atomic alloy has a special position. The Pb–Pb coordination number and the Pb–Pb distance, calculated from the first maximum of the coordination shell of the RDF, attains a minimum value for this composition. Furthermore, it has been argued that the double-peak structure of the coordination shell gives support to the idea of the formation of Pb_4 tetrahedra. A RISM calculation based on a structural unit (K_4Pb_4) that incorporates Pb_4 tetrahedra gives a reasonable description of the structural features. In both $K_{0.80}Pb_{0.20}$ and $K_{0.25}Pb_{0.75}$ indications of a tendency towards phase separation have been found.

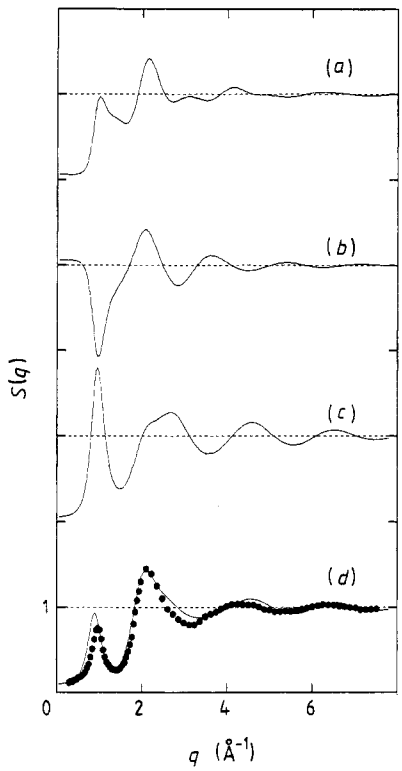

Figure 4. Results of the RISM calculations for $K_{0.50}Pb_{0.50}$. The above three plots show (*a*), the K–K partial, (*b*), the K–Pb partial, and (*c*) the Pb–Pb partial structure factor. In (*d*) the measured structure factor (dots) is compared with the total RISM structure factor (solid curve).

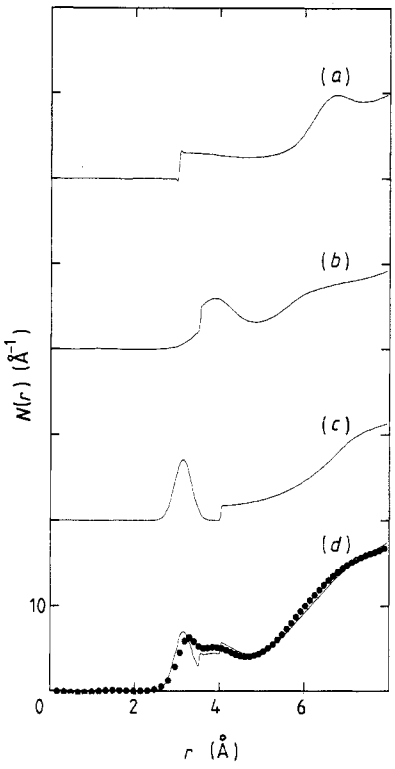

Figure 5. Radial distribution function determined by using RISM for (*a*) K–K pairs, (*b*) K–Pb pairs, and (*c*) Pb–Pb pairs. In (*d*) the total radial distribution function based on RISM (solid curve) is compared with the measurements (dots).

Acknowledgments

The authors gratefully acknowledge the technical assistance of Mr A Bontenbal during the measurements. This work forms part of the research program of the 'Stichting voor Fundamenteel Onderzoek der Materie (Foundation for Fundamental Research on Matter, FOM) and was made possible by financial support from the Nederlandse Organisatie voor Zuiver Wetenschappelijk Onderzoek (Netherlands Organisation for the Advancement of Pure Research, ZWO).

Dr M-L Saboungi gratefully acknowledges the support of the US Department of Energy, Office of Basic Energy Sciences, Division of Materials Science, under Contract W-31-109-ENG-38.

References

Alblas B P, Van de Lugt W, Dijkstra J, Geertsma W and Van Dijk C 1983 *J. Phys. F: Metal Phys.* **13** 2465
Ashcroft N W and Langreth D C 1967 *Phys. Rev.* **156** 685

Barnes A C and Enderby J E 1988 *Phil. Mag.* B **58** 497
Bermejo F J, Enciso E, Alonso J, Garcia N and Howells W S 1988 *Mol. Phys.* **64** 1169
Blech I A and Averbach B L 1965 *Phys. Rev.* A **137** 1113
Boos A, Steeb S and Godel D 1972 *Z. Naturf.* a **27** 271
Bredig M A 1964 *Molten Salt Chemistry* ed. M Blander (New York: Wiley)
Busmann E 1961 *Z. Anorg. (Allg.) Chem.* **313** 90
Chandler D and Andersen H C 1972 *J. Chem. Phys.* **57** 1930
Dahlborg U, Davidovic M and Larsson K E 1977 *Phys. Chem. Liq.* **6** 149
Geertsma W 1985 *Physica* B **132** 337
Geertsma W, Dijkstra J and Van der Lugt W 1984 *J. Phys. F: Metal Phys.* **14** 1833
Gschneider Jr K A 1961 *Rare Earth Alloys* (Princeton, NJ: Van Nostrand)
Gubbins K E, Gray C G, Egelstaff P A and Ananth M S 1973 *Mol. Phys.* **25** 1353
Hewaidy I F, Busmann E and Klemm W 1964 *Z. Anorg. (Allg.) Chem.* **328** 283
Huijben M J and Van der Lugt W 1979 *Acta Crystallogr.* A **35** 431
Jal J-F, Mathieu C, Dupuy J and Chieux P 1988 *Z. Phys. Chem. NF* **156** 189
Johnson G K and Saboungi M-L 1987 *J. Chem. Phys.* **86** 6376
Kaplow R, Strong S L, Averbach B L 1965 *Phys. Rev.* A **138** 1336
Koester L and Yelon W B 1982 *Theory of Neutron Scattering from Condensed Matter* ed. S W Lovesey (Oxford: Clarendon)
Lamparter P, Martin W and Steeb S 1984 *J. Non-Cryst. Solids* **61** 279
Lowden L J and Chandler D 1973 *J. Chem. Phys.* **59** 6587
—— 1974 *J. Chem. Phys.* **61** 5228
Marsh R E and Shoemaker D P 1953 *Acta Crystallogr.* **6** 197
Martin W, Freyland W, Lamparter P and Steeb S 1980 *Phys. Chem. Liq.* **10** 49, 61, 77
Meijer J A, Geertsma W and Van der Lugt W 1985 *J. Phys. F: Metal Phys.* **15** 899
North D M, Enderby J E and Egelstaff P A 1968 *J. Phys. C: Solid State Phys.* **1** 1075
Pings C J 1968 *Physics of Simple Liquids* ed. H N V Temperley, J S Rowlinson and G S Rushbrooke (Amsterdam: North Holland)
Placzek G 1952 *Phys. Rev.* **86** 377
Poncet P F J 1976 *PhD Thesis* University of Reading, UK
—— 1977 *Institut Laue–Langevin, Report No* 77 PO15S
Reijers H T J, Van der Lugt W and Van Dijk C 1987 *Physica* B **144** 404
Richardson J 1987 private communication
Ruppersberg H and Egger H 1975 *J. Chem. Phys.* **63** 4095
Saar J and Ruppersberg H 1988 *Z. Phys. Chem. NF* **156** 587
Saboungi M-L, Leonard S R and Ellefson J 1986 *J. Chem. Phys.* **85** 6072
Saboungi M-L, Blomquist R, Volin K J and Price D L 1987 *J. Chem. Phys.* **87** 2278
Springelkamp F, DeGroot R A, Geertsma W, Van der Lugt W and Mueller F M 1985 *Phys. Rev.* B **32** 2319
Steffen B 1976 *Phys. Rev.* B **13** 3227
Tamaki S and Cusack N E 1979 *J. Phys. F: Metal Phys.* **9** 403
Thümmel R and Klemm W 1970 *Z. Anorg. (Allg.) Chem.* **376** 44
Van der Lugt W and Meijer J 1987 *Amorphous and Liquid Materials* ed. E Lüscher, G Fritsch and G Jacucci (Dordrecht: Nijhoff)
Van der Lugt W and Geertsma W 1987 *Can. J. Phys.* **65** 326
Verlet L 1968 *Phys. Rev.* **165** 201
Waghorne R M, Rivlin V G and Williams G I 1967 *Adv. Phys.* **16** 215
Wagner C N J 1978 *J. Non-Cryst. Solids* **31** 1
Waseda Y, Yokoyama K and Suzuki K 1975 *Phys. Chem. Liq.* **4** 267
Yarnell J L, Katz M J, Wenzel R G and Koenig S H 1973 *Phys. Rev.* A **7** 2130